Kinetics of Pb Reactions with N_2O, Cl_2, HCl, and O_2 at High Temperatures

Biljana Cosic and Arthur Fontijn*

High-Temperature Reaction Kinetics Laboratory, The Isermann Department of Chemical Engineering, Rensselaer Polytechnic Institute, Troy, New York 12180-3590

Received: January 14, 2000; In Final Form: March 29, 2000

The title reactions of ground-state lead atoms have been studied in isolation in an HTFFR (high-temperature fast-flow reactor) at pressures in the 10−150 mbar range. Pb consumption rate coefficients were determined using atomic resonance absorption spectrometry at 217.0 and 283.3 nm. The following results, in cm^3 $molecule^{-1}$ s^{-1}, have been obtained: Pb + N_2O, $k(650-1205\ K) = 1.8 \times 10^{-10} \exp(-8948\ K/T)$; Pb + Cl_2, $k(530-1165\ K) = 2.3 \times 10^{-10} \exp(-718\ K/T)$; Pb + HCl, $k(1090-1320\ K) = 8.2 \times 10^{-10} \exp(-17233\ K/T)$. The precision limits vary somewhat between these measurements; the estimated 2σ accuracy limits are all about ±25%. The Pb + HCl result suggests that $D_0(Pb-Cl) = 318 \pm 31$ kJ mol^{-1}. In contrast to the above homogeneous processes, the observations on the O_2 reaction indicate the dominance of heterogeneous reactions. It is speculated that these lead primarily to PbO_2 below 1000 K and to PbO above 1000 K.

Introduction

The presence of metals in many high-temperature environments, such as waste incineration, coal combustion, and many industrial processes, can lead to toxic emissions as particles and gases. Sorbents have been developed to clean flue gases,[1] but their performance is critically dependent on the chemical form of the metals. Influencing the chemistry in a favorable direction for this approach to work again requires knowledge of the metal species kinetics. The removal of lead from gasoline notwithstanding, Pb remains one of the major elements of environmental concern.[2] Data on the kinetics of the formation of lead oxides and chlorides at combustion temperatures are much needed.[3] Most of the available information on ground state Pb(6^3P_0) reactions comes from the work of Husain and co-workers, who studied a number of reactions at room temperature[4−6] and also determined the temperature dependence of the reactions with several alkyl chlorides and SF_6 (594−819 K),[7] alkyl bromides (640−760 K),[8] and N_2O (648−783 K).[9] Husain and Littler determined rate coefficient expressions for the third-order reactions with NO and O_2 between 290 and 570 K,[10] which show a negative activation energy. Their experiments were carried out in a static tubular photochemical reactor. For Pb + O_2 + M Ryason and Smith,[11] using a quartz fast-flow reactor, obtained $k(870\ K) = 9.4 \times 10^{-33}$ cm^6 $molecule^{-2}$ s^{-1}, somewhat higher than extrapolation of Husain's results would predict. However, at that temperature the reaction was thought to be 50% due to wall reactions, which totally dominated at higher temperatures (960 and 992 K).

Here we report on four reactions of ground state lead atoms studied in a high-temperature fast-flow reactor (HTFFR) at temperatures in the range encountered in incinerators (≈700−1500 K):

$$Pb + N_2O \rightarrow PbO + N_2 \qquad \Delta H_{298} = -207 \pm 7 \text{ kJ mol}^{-1}\ ^{12} \tag{1}$$

$$Pb + Cl_2 \rightarrow PbCl + Cl \qquad \Delta H_{298} = -60 \pm 50 \text{ kJ mol}^{-1}\ ^{12} \tag{2}$$

$$Pb + HCl \rightarrow PbCl + H \qquad \Delta H_{298} = 130 \pm 50 \text{ kJ mol}^{-1}\ ^{12} \tag{3}$$

$$Pb + O_2 \rightarrow \text{products} \tag{4}$$

The inclusion of reaction 1 allows a direct comparison in an overlapping temperature interval with the results of Husain and Sealy[9] obtained by a radically different technique. Also, it provides an additional wide temperature range measurement of an activation barrier for a group 14 element, to allow future development of the SECI approach for calculating such barriers.[13−15] This approach has previously been applied to the N_2O reactions of metal atoms of the first three main groups of the periodic table, as well as to some diatomic metal oxides and halides with various oxidants. The measurements on reaction 3 have allowed a reevaluation of the heat of that reaction, as well as of reaction 2, from the above JANAF values. The O_2 results confirm the importance of heterogeneous processes in its reaction with Pb atoms.

Technique

The kinetic measurements were made in a high-temperature fast-flow reactor (HTFFR) using atomic resonance absorption spectrometry (ARAS). The apparatus, procedures, and data analysis methods have been described extensively in many earlier publications.[15−18] The reaction tube is heated radiatively by SiC resistance heating elements inside a water-cooled steel vacuum housing. Atomic Pb was generated by evaporation of solid lead from an alumina crucible. The vapor was entrained in a stream of bath gas and reacted with an oxidant, introduced through a movable inlet downstream from the Pb source. Except where otherwise mentioned, an industrial-grade quartz reaction tube and N_2 bath gas were used. Temperature was measured with a retractable Pt−Pt/13% Rh thermocouple. Pressure measurements were obtained downstream from the reaction zone using an MKS Baratron pressure transducer. Gas flow rates were determined by calibrated Hastings-Teledyne mass-flow controllers. The Pb resonance radiation was generated by a Buck Scientific hollow cathode lamp, and the absorption was measured with an Oriel monochromator equipped with a Thorn EMI

* Corresponding author. E-mail:fontia@rpi.edu.

10.1021/jp000209z CCC: $19.00
Published on Web 05/19/2000

9831QA photomultiplier tube, the output of which was transferred to a Keithley 614 electrometer. The transitions $\lambda = 217.0$ nm ($Pb(6^3D_1) \leftarrow Pb(6^3P_0)$) or $\lambda = 283.3$ nm ($Pb(7^3P_1) \leftarrow Pb(6^3P_0)$) were observed.

The gas concentrations were chosen such that [Pb] ≪ [oxidant]≪[bath gas], providing for pseudo-first-order conditions in the reaction zone. Rate coefficient measurements were performed in the stationary inlet mode[18] with reaction zone lengths of 10 or 20 cm. Individual rate coefficients, k_i, were obtained from the slope of linear plots of ln $[Pb]_{relative}$ vs [oxidant].[19] A weighted linear regression was used to determine k_i and σ_{ki}.[20] Typically, five oxidant concentrations, providing variation by a factor of 5, were used. The chemicals used were Pb granules (30 mesh, 99.5+%) from Aldrich; N_2 (99.995%) and Ar (99.998%) bath gases both from the liquid, from Praxair; N_2O (99.99%), Cl_2 (0.029% in Ar), and O_2 (99.99%), all from Matheson; and HCl (99.995%) from Spectra Gases Inc. These oxidants flowed through Drierite ($CaSO_4$) drying towers.

Results and Discussion

The Pb + N_2O Reaction. The temperature and pressure ranges covered in this study were 660−1205 K and 10−85 mbar, respectively. The low-temperature limit was determined by the small value of the rate coefficients. The high-temperature limit was imposed by thermal decomposition of nitrous oxide. In previous HTFFR work,[21,22] with Ar as bath gas, that limit was found to be around 1000 K. This study showed that with N_2 as bath gas, which helps stabilize N_2O by reducing its equilibrium dissociation,[23] the temperature limit could be increased to 1200 K.[24] The other reaction conditions including pressure and correspondingly total concentration [M], maximum N_2O concentration $[N_2O]_{max}$, observed reaction zone length z, average velocity $\bar{v}$, and initial Pb absorption were also varied; their values are listed in Table 1 together with the individual rate coefficients k_i measured. Residual analysis based on examination of $[k(T) - k_i]/k(T)$ plots showed that the rate coefficients were independent of any of the listed variables and the absorption line used. The data are well fitted by a weighted linear regression[25,26] of the form $k(T) = A \exp(-E/T)$ to yield

$$k_1(660-1205\ \mathrm{K}) = 1.76 \times 10^{-10} \exp(-8921\ \mathrm{K}/T)\ \mathrm{cm^3\ molecule^{-1}\ s^{-1}} \quad (5)$$

This activation energy is equivalent to 74 kJ mol^{-1}. The calculated variances and covariance are $\sigma_A^2 = 3.13 \times 10^{-2}$ A^2, $\sigma_E^2 = 2.50 \times 10^4$, and $\sigma_{AE} = 2.76 \times 10$ A, corresponding to $\pm 2\sigma_k$ precision limits varying from 14% at 660 K to 11% at 1205 K. Allowing ±20% for possible systematic errors and ±10% for the uncertainty associated with the flow profile factor η[1,4,18,27,28] yields $\pm 2\sigma_k$ confidence limits varying from 27% to 25%.

The reaction of Pb with N_2O was previously studied by Husain and Sealy[9] in the 648−783 K temperature interval, at pressures around 100 mbar. They used time-resolved ARAS following the pulsed irradiation of $PbBr_2$ and determined

$$k_1(648-783\ \mathrm{K}) = 6 \times 10^{-11} \exp(-8179 \pm 1203\ \mathrm{K}/T)\ \mathrm{cm^3\ molecule^{-1} s^{-1}} \quad (6)$$

There is a misprint in their Table 1, where the rate coefficients were assigned the power 10^{-11} instead of 10^{-16}. That the latter was meant can be concluded from eq 6. In Figure 1 the data sets are compared. The agreement is excellent, allowing a combined expression

$$k_1(648-1205\ \mathrm{K}) = 1.80 \times 10^{-10} \exp(-8948\ \mathrm{K}/T)\ \mathrm{cm^3\ molecule^{-1}\ s^{-1}} \quad (7)$$

Adding their individual data points to the present set, we arrive at accuracy limits equal to those of eq 5.

The pressure independence is in accord with the suggested abstraction reaction 1. These results may be compared to those of the group 14 elements Sn and Ge with N_2O, the temperature dependence of which was studied most extensively in previous HTFFR experiments to yield, respectively[21,29]

$$Sn + N_2O \rightarrow SnO + N_2 \qquad \Delta H_{298} = -365\ \mathrm{kJ\ mol^{-1}} \quad (8)$$

$$k_8(300-950\ \mathrm{K}) = 8.9 \times 10^{-13} \exp(-2260\ \mathrm{K}/T)\ \mathrm{cm^3\ molecule^{-1}\ s^{-1}}$$

$$Ge + N_2O \rightarrow GeO + N_2 \qquad \Delta H_{298} = -492\ \mathrm{kJ\ mol^{-1}} \quad (9)$$

$$k_9(475-920\ \mathrm{K}) = 1.7 \times 10^{-11} \exp(-470\ \mathrm{K}/T)\ \mathrm{cm^3\ molecule^{-1}\ s^{-1}}$$

The ground states of these group 14 elements are $^3P_0$, and their reactions with N_2O are spin-forbidden for formation of ground state products

$$Z(^3P_0) + N_2O(X^1\Sigma) \rightarrow ZO(X^1\Sigma) + N_2(X^1\Sigma) \quad (Z = Pb, Sn, Ge) \quad (10)$$

but allowed for production of triplet ZO. Spin conservation does not have to play a major role for as heavy an element as Pb, and reaction 1 is insufficiently exothermic[12,30] to populate a PbO triplet level. Indeed the preexponential of k_1 is of the same magnitude as that measured at similar temperatures for the spin-allowed N_2O reactions with Cr,[31] Cu,[32] and Al.[13]

The preexponentials of the Sn and Ge reactions are considerably smaller. These reactions, as witnessed by their chemiluminescence, are known to lead in part to triplet states.[21,29] They have been extensively discussed and compared to each other[29] and are thought to proceed through intermediate formation of $Sn(^3P_1)$ and $Ge(^3P_1)$, respectively. Indeed their activation energies compare well to the $^3P_0-^3P_1$ energy splits of 20 and 6.7 kJ mol^{-1}, respectively. This, in addition to the sequence of their reaction exothermicities,[9] has been advanced[29] as the reason for the greater activation energy for Sn compared to Ge. The lower preexponential of Sn relative to Ge has been attributed to its reaction being more selective in producing ZO to a major degree in one state, a $^3\Sigma$, resulting in a lower entropy of activation.[29]

The $Pb(6^3P_0-6^3P_1)$ split is 93.5 kJ mol^{-1}, considerably more than the Pb + N_2O activation energy. This makes it likely that this reaction proceeds directly from 6^3P_0 atoms and does not go through intermediate 6^3P_1 formation. The equilibrium population of $Pb(6^3P_1)$ also should be negligible at the temperatures investigated. Thus eq 10 appears to correctly represent the reaction path for the Pb + N_2O reaction studied, allowing for intermediate complex formation.

The Pb + Cl_2 Reaction. The rate coefficient measurements spanned the 530−1165 K temperature range. The lower temperature limit is due to the heating of the source used for Pb evaporation. The upper temperature limit was set by thermal dissociation of Cl_2, which became significant only at the temperatures above 1200 K. Residual analyses were, as above, performed to check the dependence of the rate coefficients on

TABLE 1: Summary of Rate Coefficient Measurements of Pb + N_2O[a]

T, K	*P*, mbar	[M], 10^{17} cm^{-3}	$[N_2O]_{max}$, 10^{15} cm^{-3}	$\bar{v}$, m s^{-1}	reaction zone length, cm	initial Pb absorption, %	$k_i \pm \sigma_{ki}$, cm^3 molecule^{-1} s^{-1}
722	56.0	5.62	37.2	9	20	39	$(6.41 \pm 0.44) \times 10^{-16}$
725	39.8	3.97	32.2	11	20	36	$(1.01 \pm 0.07) \times 10^{-15}$
729	39.8	3.95	32.0	12	20	36	$(9.35 \pm 0.62) \times 10^{-16}$
904	70.6	5.65	22.5	8	20	37	$(9.46 \pm 0.57) \times 10^{-15}$
987	23.4	1.72	8.5	26	20	42	$(2.29 \pm 0.19) \times 10^{-14}$
988	23.4	1.72	8.5	26	10	45	$(2.10 \pm 0.17) \times 10^{-14}$
978	65.5	4.85	23.9	9	10	23	$(1.24 \pm 0.09) \times 10^{-14}$
971	65.6	4.90	17.2	9	20	45	$(1.41 \pm 0.09) \times 10^{-14}$
799	34.6	3.14	15.5	14	20	46	$(2.59 \pm 0.18) \times 10^{-15}$
784	34.8	3.21	23.2	14	20	36	$(2.43 \pm 0.17) \times 10^{-15}$
762	76.8	7.30	52.7	6	20	43	$(1.23 \pm 0.07) \times 10^{-15}$
892	17.8	1.44	10.4	31	20	48	$(9.25 \pm 0.87) \times 10^{-15}$
881	40.0	3.29	23.8	14	10	39	$(6.37 \pm 0.46) \times 10^{-15}$
880	40.0	3.29	23.8	14	10	37	$(6.38 \pm 0.45) \times 10^{-15}$
752	40.1	3.86	27.9	12	20	39	$(1.45 \pm 0.10) \times 10^{-15}$
749	85.9	8.31	48.7	5	20	41	$(1.08 \pm 0.06) \times 10^{-15}$
693	68.9	7.20	41.8	6	20	28	$(3.58 \pm 0.21) \times 10^{-16}$
700	35.6	3.68	29.6	12	20	32	$(6.48 \pm 0.51) \times 10^{-16}$
700	48.2	4.99	47.2	8	20	32	$(4.60 \pm 0.34) \times 10^{-16}$
675	48.2	5.18	49.0	8	20	30	$(2.46 \pm 0.17) \times 10^{-16}$
673	69.7	7.50	71.0	5	20	26	$(2.40 \pm 0.15) \times 10^{-16}$
1205	10.2	0.62	2.0	80	20	31	$(1.31 \pm 0.20) \times 10^{-13}$
1201	12.0	0.72	2.7	81	20	26	$(9.25 \pm 1.35) \times 10^{-14}$
1191	11.0	0.67	2.8	80	20	22	$(9.67 \pm 1.38) \times 10^{-14}$
1162	19.5	1.21	5.5	41	20	47	$(8.17 \pm 0.78) \times 10^{-14}$
1160	19.6	1.22	8.1	41	10	52	$(6.22 \pm 0.59) \times 10^{-14}$
1075	31.1	2.10	6.8	23	20	32	$(5.32 \pm 0.40) \times 10^{-14}$
1074	17.3	1.16	3.7	42	20	43	$(6.30 \pm 0.60) \times 10^{-14}$
1064	41.6	2.83	6.6	17	10	30	$(3.92 \pm 0.30) \times 10^{-14}$
1051	41.6	2.87	6.7	17	10	26	$(3.87 \pm 0.30) \times 10^{-14}$
892	30.4	2.47	11.5	19	20	39	$(7.18 \pm 0.51) \times 10^{-15}$
903	30.4	2.44	11.4	20	20	40	$(8.39 \pm 0.60) \times 10^{-15}$
898	57.4	4.63	13.3	10	20	30	$(7.47 \pm 0.45) \times 10^{-15}$
906	52.4	4.19	12.1	11	20	33	$(7.94 \pm 0.51) \times 10^{-15}$
840	52.5	4.53	21.2	11	20	36	$(3.44 \pm 0.23) \times 10^{-15}$
833	18.3	1.59	10.9	30	20	44	$(4.77 \pm 0.44) \times 10^{-15}$
847	71.4	6.10	24.3	9	10	21	$(3.54 \pm 0.25) \times 10^{-15}$
743	49.2	4.79	34.4	10	20	54[b]	$(1.11 \pm 0.08) \times 10^{-15}$
743	49.2	4.79	34.4	10	20	40[b]	$(1.22 \pm 0.08) \times 10^{-15}$
741	49.2	4.81	34.5	9	20	38[b]	$(1.37 \pm 0.09) \times 10^{-15}$
1095	49.5	3.27	5.1	14	10	56[b]	$(4.33 \pm 0.33) \times 10^{-14}$
1094	18.1	1.20	5.9	38	10	52[b]	$(6.48 \pm 0.71) \times 10^{-14}$
663	33.8	3.69	29.8	12	20	42	$(3.03 \pm 0.24) \times 10^{-16}$
661	27.7	3.03	30.1	12	20	40	$(2.42 \pm 0.19) \times 10^{-16}$
813	37.6	3.35	16.5	14	20	51[b]	$(3.35 \pm 0.27) \times 10^{-15}$
1048	21.8	1.51	7.4	30	20	49[b]	$(4.37 \pm 0.44) \times 10^{-14}$
1043	22.1	1.54	3.9	29	20	17	$(3.07 \pm 0.26) \times 10^{-14}$
1043	22.1	1.54	3.9	29	20	55[b]	$(3.56 \pm 0.32) \times 10^{-14}$
877	32.8	2.71	13.4	17	20	24	$(7.84 \pm 0.68) \times 10^{-15}$
839	28.4	2.45	12.1	18	20	53[b]	$(4.08 \pm 0.30) \times 10^{-15}$
982	28.4	2.09	10.4	22	20	33[b]	$(2.26 \pm 0.20) \times 10^{-14}$
1036	28.4	1.98	9.8	23	20	57[b]	$(2.91 \pm 0.21) \times 10^{-14}$

[a] The measurements are reported in the sequence in which they were obtained. [b] The 217.0 nm absorption line was used in these experiments. In all other experiments the 283.3 nm line was used.

the reaction parameters. Originally, the pressure range used was 10−65 mbar; however, the data at the highest pressures were systematically lower than those from 20 to 50 mbar, and those at the lowest pressures were systematically higher. Only data in this central range, which are independent of the reaction parameters, were retained; cf. Table 2. Because of this problem a few further factors were considered. First, Cl_2 has a wide absorption continuum extending from the visible region to 250 nm with a maximum around 330 nm,[30] which could have affected the 283 nm measurements. However, in experiments without Pb no absorption by Cl_2 could be observed at the concentrations used. [Cl_2] several orders of magnitude higher were required to begin to observe absorption. The data may be seen to be independent of the absorption line used; cf. also Figure 2. Second, it was investigated if the flow profile factor could have influenced the results at the extremes of pressure. However, residual plots of the rate coefficients versus the Reynolds number $Re = (2\bar{v}aP)/(\nu RT)$ [33] of the individual experiments showed no dependence. Thus this is not a factor.

The data were fitted by a weighted linear regression, as above, to yield

$$k_2(530-1165\ \mathrm{K}) = 2.28 \times 10^{-10} \exp(-718\ \mathrm{K}/T)\ \mathrm{cm}^3\ \mathrm{molecule}^{-1}\ \mathrm{s}^{-1} \quad (11)$$

where the 718 K corresponds to 5.97 kJ mol^{-1}. The variances and covariance are $\sigma_A^2 = 4.21 \times 10^{-3}$ A^2, $\sigma_E^2 = 2.76 \times 10^3$, and $\sigma_{AE} = 3.33$ A. The $\pm 2\sigma_k$ precision limits are determined to be 8% at 534 K and 5% at 1186 K yielding confidence limits of 24% and 23%.

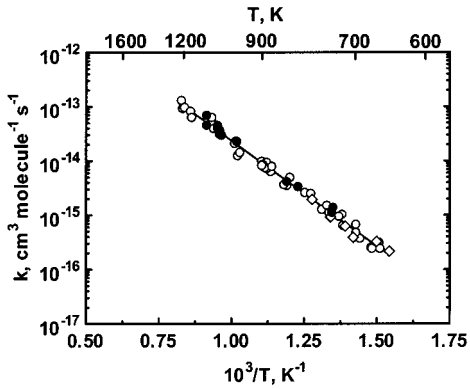

Figure 1. Arrhenius plot of the Pb + N_2O rate coefficients: (○) measurements taken at 283.3 nm; (●) measurements taken at 217.0 nm; (◇) Husain and Sealy; (—) best fit to the joint measurements (eq 7).

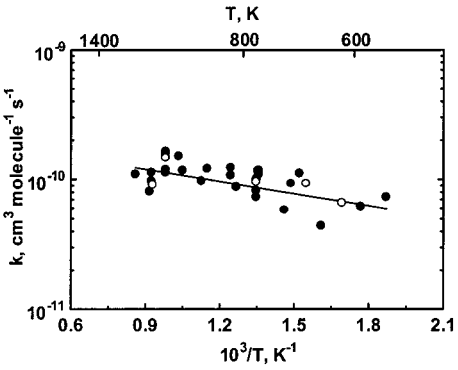

Figure 2. Arrhenius plot of the Pb + Cl_2 rate coefficients: (●) measurements taken at 217.0 nm; (○) measurements taken at 283.3 nm; (—) best fit to the measurements (eq 11).

The large preexponential and rather small activation energy of eq 11 are typical for exothermic Cl_2 reactions with metal atoms. Several have thus far been measured over a range of temperatures, i.e., those with Al,[34] Cr,[31] Mg,[35] Ti,[36] and Cu.[37] All these are thought to proceed by abstraction, which is also thought to be the dominant mechanism for Pb; cf. eq 2.

The Pb + HCl Reaction. The reaction rates for this system could only be obtained in the narrow temperature range 1090−1320 K. At lower temperatures the rates were too low to be measurable, and above about 1320 K the drop in the observed reaction rate coefficients indicated thermal decomposition of the relatively weakly bound product PbCl (see below). The rate coefficients fall within the $(1-20) \times 10^{-16}$ cm^3 molecule^{-1} s^{-1} range, which largely is lower than could be achieved in previous HTFFR studies. Accordingly, they show a larger scatter than those from the N_2O and Cl_2 reactions; cf. Figure 3. The residual analysis shows the data to be independent of the reaction parameters, Table 3. Linear regression yields

$$k_3(1090-1320\ \mathrm{K}) = 8.22 \times 10^{-10} \exp(-17233\ \mathrm{K}/T)\ \mathrm{cm}^3\ \mathrm{molecule}^{-1}\ \mathrm{s}^{-1} \quad (12)$$

where 17233 K is equivalent to 143 kJ mol^{-1}. The variances

TABLE 2: Summary of Rate Coefficient Measurements of Pb + Cl_2[a]

T, K	P, mbar	[M], 10^{17} cm^{-3}	$[Cl_2]_{max}$, 10^{12} cm^{-3}	$\bar{v}$, m s^{-1}	reaction zone length, cm	initial Pb absorption, %	$k_i \pm \sigma_{ki}$, cm^3 molecule^{-1} s^{-1}
742	52.0	5.08	2.63	12	20	25	$(9.53 \pm 0.60) \times 10^{-11}$
742	52.0	5.08	5.06	13	10	25[b]	$(7.35 \pm 0.48) \times 10^{-11}$
742	34.6	3.37	3.36	19	10	33[b]	$(9.99 \pm 0.72) \times 10^{-11}$
741	34.7	3.39	5.28	19	10	27[b]	$(1.02 \pm 0.08) \times 10^{-10}$
736	34.4	3.39	1.76	19	20	33[b]	$(1.18 \pm 0.08) \times 10^{-10}$
1017	46.9	3.34	1.41	19	20	34[b]	$(1.58 \pm 0.10) \times 10^{-10}$
1020	46.9	3.33	3.32	19	10	30[b]	$(1.14 \pm 0.08) \times 10^{-10}$
1017	46.9	3.34	3.33	19	10	30[b]	$(1.20 \pm 0.09) \times 10^{-10}$
1018	28.5	2.03	2.02	31	10	37[b]	$(1.65 \pm 0.13) \times 10^{-10}$
1018	28.7	2.04	3.92	31	10	31[b]	$(1.59 \pm 0.13) \times 10^{-10}$
1019	28.7	2.04	3.92	31	10	61	$(1.47 \pm 0.12) \times 10^{-10}$
1019	28.7	2.04	3.92	31	10	59[b]	$(1.49 \pm 0.12) \times 10^{-10}$
534	50.9	6.91	2.91	9	20	23[b]	$(7.30 \pm 0.68) \times 10^{-11}$
742	30.9	3.02	6.80	18	20	62[b]	$(8.26 \pm 0.80) \times 10^{-11}$
738	36.5	3.58	10.0	18	10	48[b]	$(1.17 \pm 0.08) \times 10^{-10}$
738	36.5	3.58	6.87	18	10	57[b]	$(1.16 \pm 0.09) \times 10^{-10}$
737	36.1	3.55	3.53	18	10	67[b]	$(1.10 \pm 0.09) \times 10^{-10}$
1081	34.5	2.31	5.17	24	20	49[b]	$(9.68 \pm 0.70) \times 10^{-11}$
1080	34.2	2.30	2.67	24	20	46[b]	$(1.14 \pm 0.09) \times 10^{-10}$
1079	34.1	2.29	1.12	24	20	46	$(9.16 \pm 0.67) \times 10^{-11}$
1089	48.7	3.24	1.59	17	20	32[b]	$(8.06 \pm 0.55) \times 10^{-11}$
622	27.7	3.22	7.11	17	20	43[b]	$(4.39 \pm 0.35) \times 10^{-11}$
646	44.5	4.87	6.59	12	20	28	$(9.35 \pm 1.02) \times 10^{-11}$
658	23.1	2.94	3.40	24	20	23[b]	$(1.11 \pm 0.20) \times 10^{-10}$
673	41.4	4.46	2.13	19	20	33[b]	$(9.33 \pm 0.95) \times 10^{-11}$
790	52.0	5.97	2.55	12	10	25[b]	$(8.88 \pm 0.99) \times 10^{-11}$
803	37.5	4.11	1.82	25	20	31[b]	$(1.07 \pm 0.10) \times 10^{-10}$
804	30.8	3.84	1.60	31	20	34[b]	$(1.23 \pm 0.11) \times 10^{-10}$
591	49.5	7.12	2.99	10	20	39	$(6.58 \pm 0.58) \times 10^{-11}$
566	24.9	3.28	1.59	24	20	45[b]	$(6.23 \pm 0.60) \times 10^{-11}$
889	29.4	2.48	2.88	27	20	39[b]	$(9.69 \pm 0.81) \times 10^{-11}$
870	22.8	1.92	5.93	47	20	38[b]	$(1.22 \pm 0.10) \times 10^{-10}$
685	48.2	4.13	4.45	12	20	40[b]	$(5.83 \pm 0.49) \times 10^{-11}$
1163	35.9	2.28	2.57	26	20	45[b]	$(1.10 \pm 0.10) \times 10^{-10}$
965	21.0	1.52	3.09	46	10	45[b]	$(1.51 \pm 0.12) \times 10^{-10}$
951	41.7	3.06	3.41	22	20	35[b]	$(1.17 \pm 0.10) \times 10^{-10}$

[a] The measurements are reported in the sequence in which they were obtained. [b] The 217.0 nm absorption line was used in these experiments. In all other experiments the 283.3 nm line was used.

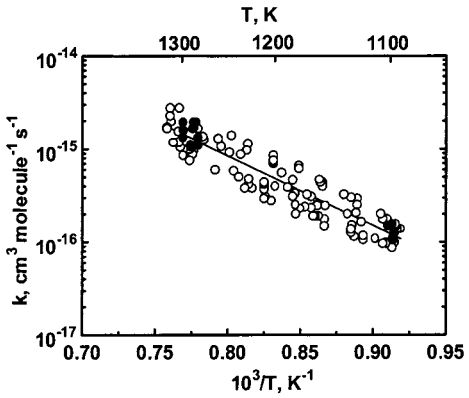

Figure 3. Arrhenius plot of the Pb + HCl rate coefficients: (●) measurements taken at 217.0 nm; (○) measurements taken at 283.3 nm; (—) best fit to the measurements (eq 12).

and covariance are $\sigma_A^2 = 2.03 \times 10^{-1}$ A^2, $\sigma_E^2 = 2.92 \times 10^5$, and $\sigma_{AE} = 2.43 \times 10^3$ A. The $\pm 2\sigma_k$ precision limits are 11% at 1090 K and 10% at 1315 K, with corresponding confidence limits of 25% and 24%, when allowing for systematic errors.

Temperature-dependent rate coefficient studies have been made for HCl reactions with K,[38] Na,[39,40] Li,[41] Al,[34] Cr,[31] and Cu[42] atoms. All have preexponentials in the about $10^{-10}-10^{-9}$ cm^3 molecule^{-1} s^{-1} range and are assumed to be abstraction reactions. This path may also be assumed for reaction 3. However, in the study of the Cu + HCl reaction, which showed the rate coefficients to be pressure independent, it was shown that an insertion product HCuCl also formed, from a second minor channel beyond the reaction barrier. The pressure-independence of the Pb and other polyvalent atom reactions may thus not guarantee that the metal chloride is the only product. Orbital symmetry calculations are helpful in deciding whether insertion could occur.[43] These suggest that HPbCl formation from reaction 3 and Cl−Pb−Cl formation from reaction 2 are possible.[44] Further investigation would have to establish if such processes occur.

The measured activation energy of reaction 3 of 143 ± 4 kJ mol^{-1} puts an upper limit on its endothermicity of 136 ± 50 kJ mol^{-1} at 1205 K,[12] the midpoint of the temperature range over which k was measured. From this and the enthalpy values from the JANAF tables,[12] an improved value of −4.4 ± 31 kJ mol^{-1} can be recovered for $\Delta_f H_{298}$(PbCl,g). This leads to an increase in D_0(Pb−Cl) from[12] 299 ± 48 to 318 ± 31 kJ mol^{-1}. The enthalpy for reaction 2 accordingly is reassessed to be −79 ± 31 kJ mol^{-1}. A factor to be considered in the use of these new figures is the presence of vibrationally excited HCl and its possible effect on the apparent activation energy. Vibrational enhancement of a reaction may become significant at high temperatures, which can result in a sudden upward curvature in Arrhenius plots.[32] Assuming equilibrium, the first and the second excited states of HCl ($v = 1, 2$), with energies of 33.3 and 65.4 kJ mol^{-1} respectively,[12] together represent 2.5% at 1090 K and 4.8% at 1315 K of the HCl population. Although the concentration of vibrationally excited species thus almost doubles over this temperature range, there is no indication of curvature in the Arrhenius plot, suggesting no substantial influence on the kinetics. If vibrational enhancement is significant, but could not be detected due to the narrowness of the temperature range, the actual E_a for HCl($v = 0$) would only be smaller. In that case the figures given above would require further corrections, the enthalpy of formation of PbCl being smaller than the suggested −4.4 kJ mol^{-1} and the bond dissociation energy larger than 318 kJ mol^{-1}.

The Pb + O_2 Reaction. Properly linear ln [Pb]$_{rel}$ versus [O_2] plots could only be obtained for limited reaction conditions. These were (i) from 660 to 920 K over narrow ranges of [M], $(0.95-1.3) \times 10^{18}$ cm^{-3}, and $\bar{v}$ 5−7 m s^{-1} and (ii) from 1010 to 1340 K also over a narrow range of [M], $(6.2-8.8) \times 10^{16}$ cm^{-3}, and a somewhat wider range of $\bar{v}$, 65−129 m s^{-1}. Use of a mullite reaction tube and Ar as bath gas led to within experimental error to the same results; cf. Tables 4S and 5S in the Supporting Information. These are indications that observations are not predominantly for homogeneous processes, which is in agreement with the results of Ryason and Smith[11] mentioned above.

The lower temperature rate coefficients have a negative temperature dependence, Figure 4a. Linear regression yields $k_{4,l}(660-920\ \text{K}) = 2.2 \times 10^{-17} \exp(2330\ \text{K}/T)$ cm^3 molecule^{-1} s^{-1}. Residual analysis does not show any definite dependence on the reaction condition parameters, although because of the narrow ranges some dependence would probably not show. The lack of an [M] dependence indicates that this is not a homogeneous addition reaction. Such reactions for a simple triatomic system could not be at their high-pressure limit at these temperatures. The abstraction reaction

$$\text{Pb} + \text{O}_2 \rightarrow \text{PbO} + \text{O} \qquad (13)$$

would be 124 ± 7 kJ mol^{-1} endothermic[12] and thus have rate coefficients $< 1 \times 10^{-16}$ cm^3 molecule^{-1} s^{-1}, too slow to be measurable in this temperature range. Yet, a slow reaction with rate coefficients $(3-8) \times 10^{-16}$ cm^3 molecule^{-1} s^{-1} occurs, suggesting a heterogeneous process. The aforementioned Husain and Littler[10] results show very different Arrhenius factors for the three bath gases used, He, CO_2, and C_2H_6. Though there is considerable uncertainty in their data, the strong dependence on the nature of M could indicate participation of a PbM + O_2 type of three-body mechanism, rather than the more common energy-transfer process. In that case the function of M at higher temperatures apparently gets substituted by the walls. Ryason and Smith interpreted their 870 K data as being in part due to homogeneous reaction.[11] Their 9.4×10^{-33} cm^6 molecule^{-2} s^{-1} is about 2 orders of magnitude higher than $k_{4,l}$/[M] at that temperature. However, the wide scatter shown in their k_{obs}/[O_2] vs [Ar] plot makes it doubtful that any meaningful data could have been obtained from their measurements. Their[11] and our measurements may be taken as phenomenological for the particular reactors used. It may be concluded that

$$\text{Pb} + \text{O}_2 \xrightarrow{\text{wall}} \text{PbO}_2 \qquad (14)$$

is the likely dominant mechanism observed in the 660−920 K range.

The higher temperature data show a positive temperature dependence; cf. Figure 4b. Linear regression leads to $k_{4,h}(1010-1340\ \text{K}) = 3.4 \times 10^{-12} \exp(-4823\ \text{K}/T)$ cm^3 molecule^{-1} s^{-1}. Residual analysis does not show any definite dependence on the reaction parameters, which might suggest the homogeneous reaction 13. However, in addition to the discussed factors arguing against this possibility, the above activation energy corresponds to only 40 kJ mol^{-1}, much less than the endothermicity. This indicates a wall-catalyzed reaction. As the difference in temperature dependence from the lower temperature data would suggest a change in mechanism, one may speculate that the observed higher-temperature process is

$$\text{Pb} + \text{O}_2 \xrightarrow{\text{wall}} \text{PbO} + \text{O} \qquad (15)$$

TABLE 3: Summary of Rate Coefficient Measurements of Pb + HCl[a]

T, K	P, mbar	[M], 10^{17}cm^{-3}	[HCl]$_{max}$, 10^{16} cm^{-3}	$\bar{v}$, m s^{-1}	reaction zone length, cm	initial Pb absorption, %	$k_i \pm \sigma_{ki}$, cm^3 molecule^{-1} s^{-1}
1194	44.3	2.68	2.76	19	20	30	$(5.46 \pm 0.39) \times 10^{-16}$
1178	44.3	2.72	2.56	17	20	19	$(6.16 \pm 0.69) \times 10^{-16}$
1183	34.7	2.12	2.00	22	20	46	$(4.61 \pm 0.54) \times 10^{-16}$
1178	132.0	8.11	7.64	6	20	33	$(6.66 \pm 0.39) \times 10^{-16}$
1088	107.7	7.17	6.96	6	20	30	$(1.38 \pm 0.10) \times 10^{-16}$
1092	58.0	3.85	3.73	12	20	42	$(1.52 \pm 0.11) \times 10^{-16}$
1092	136.6	9.06	8.79	5	20	31	$(1.56 \pm 0.12) \times 10^{-16}$
1091	93.3	6.19	6.01	7	20	36	$(1.36 \pm 0.08) \times 10^{-16}$
1203	76.3	4.59	4.27	10	20	51	$(7.48 \pm 1.04) \times 10^{-16}$
1203	100.3	6.04	5.61	8	20	50	$(7.32 \pm 0.62) \times 10^{-16}$
1203	142.0	8.55	7.94	6	20	43	$(8.56 \pm 0.72) \times 10^{-16}$
1203	90.5	5.45	5.06	9	20	46	$(6.88 \pm 0.67) \times 10^{-16}$
1158	91.0	5.69	5.29	8	20	39	$(4.68 \pm 0.33) \times 10^{-16}$
1157	138.6	8.67	8.06	5	20	30	$(4.43 \pm 0.37) \times 10^{-16}$
1156	111.2	6.96	6.47	7	20	32	$(4.02 \pm 0.35) \times 10^{-16}$
1156	66.4	4.16	3.86	11	20	35	$(4.41 \pm 0.39) \times 10^{-16}$
1228	45.1	2.66	3.53	15	20	8	$(1.12 \pm 0.12) \times 10^{-15}$
1230	46.0	2.71	3.60	15	20	8	$(9.67 \pm 0.67) \times 10^{-16}$
1314	55.2	3.04	4.04	13	20	28	$(1.95 \pm 0.17) \times 10^{-15}$
1305	61.3	3.40	4.52	12	20	25	$(1.54 \pm 0.13) \times 10^{-15}$
1136	141.3	9.13	8.69	5	20	49	$(3.21 \pm 0.20) \times 10^{-16}$
1130	74.0	4.78	4.55	10	20	48	$(2.97 \pm 0.20) \times 10^{-16}$
1124	122.4	7.88	7.50	6	20	44	$(2.52 \pm 0.18) \times 10^{-16}$
1124	98.3	6.33	6.03	7	20	45	$(2.94 \pm 0.29) \times 10^{-16}$
1304	104.8	5.82	3.78	8	20	41	$(2.73 \pm 0.17) \times 10^{-15}$
1315	85.0	4.68	3.05	10	20	50	$(2.73 \pm 0.16) \times 10^{-15}$
1315	137.3	7.56	3.51	6	20	47	$(2.23 \pm 0.15) \times 10^{-15}$
1288	88.0	4.95	3.22	9	20	48	$(1.91 \pm 0.12) \times 10^{-15}$
1283	88.0	4.97	3.23	9	20	42	$(1.64 \pm 0.10) \times 10^{-15}$
1277	89.7	5.09	3.31	9	20	39	$(1.35 \pm 0.10) \times 10^{-15}$
1276	130.6	7.41	3.44	6	20	31	$(1.25 \pm 0.08) \times 10^{-15}$
1246	132.0	7.67	3.56	6	20	15	$(1.38 \pm 0.08) \times 10^{-15}$
1236	84.4	4.94	2.29	9	20	16	$(8.85 \pm 0.85) \times 10^{-16}$
1104	128.4	8.42	8.25	6	20	38	$(2.00 \pm 0.22) \times 10^{-16}$
1099	95.8	6.31	6.18	7	20	41	$(1.74 \pm 0.18) \times 10^{-16}$
1103	145.0	9.52	9.33	5	20	37	$(1.78 \pm 0.19) \times 10^{-16}$
1092	145.3	9.82	9.61	5	20	28	$(1.45 \pm 0.11) \times 10^{-16}$
1248	138.6	8.04	7.64	6	20	39	$(9.28 \pm 0.76) \times 10^{-16}$
1257	138.6	7.99	7.59	6	20	40	$(1.06 \pm 0.08) \times 10^{-15}$
1181	121.2	7.43	7.06	6	20	23	$(3.32 \pm 0.31) \times 10^{-16}$
1183	140.5	8.60	8.17	5	20	20	$(3.06 \pm 0.23) \times 10^{-16}$
1212	142.2	8.50	4.48	5	20	19	$(3.97 \pm 0.24) \times 10^{-16}$
1212	141.3	8.44	4.45	5	20	19	$(4.22 \pm 0.27) \times 10^{-16}$
1212	62.4	3.73	3.54	12	20	28	$(3.71 \pm 0.24) \times 10^{-16}$
1212	146.6	8.76	8.32	5	20	20	$(4.42 \pm 0.25) \times 10^{-16}$
1160	121.0	7.56	7.17	6	20	25	$(2.47 \pm 0.17) \times 10^{-16}$
1160	142.4	8.89	8.43	5	20	23	$(2.53 \pm 0.17) \times 10^{-16}$
1166	124.0	7.70	7.30	6	20	27	$(2.33 \pm 0.13) \times 10^{-16}$
1172	97.0	6.00	5.69	8	20	31	$(2.39 \pm 0.15) \times 10^{-16}$
1318	111.3	6.12	5.80	8	20	43	$(1.67 \pm 0.11) \times 10^{-15}$
1318	112.9	6.20	5.88	7	20	44	$(1.69 \pm 0.10) \times 10^{-15}$
1292	135.4	7.59	4.31	7	20	21	$(1.03 \pm 0.06) \times 10^{-15}$
1292	136.6	7.66	4.35	7	20	20	$(1.00 \pm 0.06) \times 10^{-15}$
1287	136.6	7.69	5.22	7	10	23	$(9.63 \pm 0.62) \times 10^{-16}$
1304	136.2	7.57	7.14	6	20	27	$(1.18 \pm 0.10) \times 10^{-15}$
1289	138.0	7.75	5.65	8	20	16	$(8.75 \pm 0.54) \times 10^{-16}$
1303	71.7	3.99	3.66	12	10	46	$(1.04 \pm 0.08) \times 10^{-15}$
1311	71.7	3.96	3.64	12	20	48	$(1.17 \pm 0.09) \times 10^{-15}$
1227	106.6	6.29	5.11	9	20	51	$(4.21 \pm 0.31) \times 10^{-16}$
1227	106.6	6.29	5.11	9	20	53	$(4.70 \pm 0.27) \times 10^{-16}$
1238	136.6	7.99	7.60	7	10	47	$(4.96 \pm 0.40) \times 10^{-16}$
1244	137.0	7.98	7.58	7	20	44	$(5.79 \pm 0.47) \times 10^{-16}$
1263	73.0	4.19	3.99	11	20	49	$(6.02 \pm 0.49) \times 10^{-16}$
1093	138.4	9.17	9.56	5	20	38	$(9.88 \pm 0.72) \times 10^{-17}$
1093	138.4	9.17	9.56	5	20	39	$(1.00 \pm 0.07) \times 10^{-16}$
1100	111.7	7.35	7.67	7	20	44	$(9.48 \pm 0.65) \times 10^{-17}$
1100	111.7	7.35	7.67	7	20	45	$(9.80 \pm 1.03) \times 10^{-17}$
1103	110.6	7.26	6.49	7	20	47	$(9.59 \pm 0.71) \times 10^{-17}$
1119	110.2	7.13	6.37	7	20	46	$(1.17 \pm 0.07) \times 10^{-16}$
1119	81.8	5.30	4.73	9	20	52	$(1.07 \pm 0.14) \times 10^{-16}$
1127	81.8	5.26	4.70	9	20	53	$(1.15 \pm 0.08) \times 10^{-16}$
1130	121.3	7.77	6.95	6	20	49	$(1.27 \pm 0.11) \times 10^{-16}$
1130	138.1	8.85	7.91	6	20	48	$(1.36 \pm 0.09) \times 10^{-16}$

TABLE 3 (Continued)

T, K	*P*, mbar	[M], 10^{17}cm^{-3}	$[HCl]_{max}$, 10^{16} cm^{-3}	$\bar{v}$, m s^{-1}	reaction zone length, cm	initial Pb absorption, %	$k_i \pm \sigma_{ki}$, cm^3 molecule^{-1} s^{-1}
1154	138.2	8.67	7.75	6	20	33	$(1.78 \pm 0.11) \times 10^{-16}$
1154	81.3	5.10	4.56	10	20	43	$(1.48 \pm 0.18) \times 10^{-16}$
1162	81.0	5.05	4.51	10	20	44	$(1.89 \pm 0.11) \times 10^{-16}$
1164	132.1	8.22	6.69	7	20	31	$(1.91 \pm 0.11) \times 10^{-16}$
1159	132.9	8.30	6.76	7	10	32	$(1.90 \pm 0.24) \times 10^{-16}$
1177	133.3	8.20	6.68	7	10	39	$(2.30 \pm 0.24) \times 10^{-16}$
1181	134.0	8.21	6.69	7	20	38	$(2.48 \pm 0.23) \times 10^{-16}$
1180	107.3	6.59	5.36	8	20	41	$(2.00 \pm 0.17) \times 10^{-16}$
1204	107.2	6.45	5.25	8	20	50	$(2.81 \pm 0.23) \times 10^{-16}$
1211	82.9	4.96	4.04	11	20	45	$(3.05 \pm 0.26) \times 10^{-16}$
1212	83.2	4.97	4.05	11	20	45	$(2.96 \pm 0.28) \times 10^{-16}$
1232	82.9	4.87	3.97	11	20	38	$(3.81 \pm 0.48) \times 10^{-16}$
1224	135.7	8.03	6.54	7	10	32	$(3.74 \pm 0.28) \times 10^{-16}$
1299	105.9	5.90	4.81	9	20	49	$(1.00 \pm 0.06) \times 10^{-15}$
1292	115.3	6.46	5.73	9	10	45	$(7.47 \pm 0.57) \times 10^{-16}$
1300	115.7	6.45	5.71	9	20	40	$(8.56 \pm 0.63) \times 10^{-16}$
1260	101.3	5.82	4.39	10	20	51	$(1.27 \pm 0.07) \times 10^{-15}$
1188	101.3	6.18	4.66	9	20	31	$(3.91 \pm 0.42) \times 10^{-16}$
1153	102.1	6.41	4.84	9	20	34	$(2.43 \pm 0.17) \times 10^{-16}$
1170	60.1	3.72	3.01	15	20	51	$(3.27 \pm 0.59) \times 10^{-16}$
1166	121.3	7.53	6.10	7	20	42	$(3.04 \pm 0.27) \times 10^{-16}$
1201	121.3	7.31	5.92	7	20	37	$(3.95 \pm 0.32) \times 10^{-16}$
1095	122.6	8.11	6.56	7	20	38	$(8.69 \pm 0.75) \times 10^{-17}$
1109	120.0	7.83	6.34	7	20	44	$(1.09 \pm 0.12) \times 10^{-16}$
1121	116.1	7.50	6.07	7	20	47	$(1.61 \pm 0.10) \times 10^{-16}$
1133	112.0	7.16	5.79	8	20	52	$(2.02 \pm 0.12) \times 10^{-16}$
1129	115.7	7.42	6.00	7	20	48	$(1.52 \pm 0.10) \times 10^{-16}$
1125	144.5	9.30	7.53	6	20	32	$(2.05 \pm 0.21) \times 10^{-16}$
1285	62.37	4.69	4.21	10	20	46[b]	$(1.90 \pm 0.27) \times 10^{-15}$
1288	95.58	7.17	2.94	5	20	63[b]	$(1.70 \pm 0.09) \times 10^{-15}$
1283	97.23	7.32	6.05	5	10	61[b]	$(1.30 \pm 0.08) \times 10^{-15}$
1283	106.33	8.01	6.63	5	10	61[b]	$(1.10 \pm 0.07) \times 10^{-15}$
1289	106.10	7.95	3.23	5	20	58[b]	$(1.60 \pm 0.09) \times 10^{-15}$
1290	76.36	5.72	6.52	7	10	70[b]	$(1.00 \pm 0.07) \times 10^{-15}$
1291	77.22	5.78	6.60	7	10	61[b]	$(1.10 \pm 0.07) \times 10^{-15}$
1299	76.78	5.71	3.18	7	20	61[b]	$(1.60 \pm 0.09) \times 10^{-15}$
1300	69.60	5.17	2.89	7	20	61[b]	$(1.90 \pm 0.12) \times 10^{-15}$
1300	85.32	6.34	3.54	6	20	61[b]	$(1.30 \pm 0.08) \times 10^{-15}$
1095	70.28	6.20	7.06	6	20	42[b]	$(1.60 \pm 0.12) \times 10^{-16}$
1098	72.11	6.35	7.07	6	20	40[b]	$(1.50 \pm 0.10) \times 10^{-16}$
1093	105.29	9.31	9.62	5	10	40[b]	$(1.20 \pm 0.09) \times 10^{-16}$
1094	104.28	9.21	9.71	5	10	41[b]	$(1.10 \pm 0.07) \times 10^{-16}$
1094	104.28	9.21	9.71	5	10	41[b]	$(1.10 \pm 0.07) \times 10^{-16}$

[a] The measurements are reported in the sequence in which they were obtained. [b] The 217.0 nm absorption line was used in these experiments. In all other experiments the 283.3 nm line was used.

The activation energy for the equivalent homogeneous reaction 13 is likely to be higher than the 124 ± 7 kJ mol^{-1} figure, based on observations of the reverse process. Golomb and Best released tetraethyllead at 100−150 km altitude from a sounding rocket. The resulting sunlight-induced PbO fluorescence persisted for a considerable time, indicating PbO reaction with O atoms to be slow.[45] Oldenborg et al.[46] argued from this, and consideration of the reaction path, that a barrier is present. They concluded that the ground-state process

$$PbO(X^1\Sigma) + O(^3P) \rightarrow Pb(^3P) + O_2(X^3\Sigma_g^-) \qquad (16)$$

should proceed on a triplet surface, with the PbO_2 triplet intermediate lying above its singlet ground state.

Two other metal oxidation reactions, studied in the temperature range of the present work, have shown a change from a (third order) association reaction at low temperatures to a predominantly (second order) abstraction reaction at high temperatures. These are Cr + O_2, for which abstraction is 40 ± 42 kJ mol^{-1} endothermic, studied[47] from 290 to 1510 K and AlO + O_2, for which abstraction is 96 ± 40 kJ mol^{-1} endothermic, and which was studied[48] from 305 to 1690 K. In that respect the Pb + O_2 system thus may be similar. However, there was no evidence for a heterogeneous component in those reactions. The rate coefficients obtained there were several orders of magnitude higher than that obtained for Pb + O_2 at comparable temperatures, which would dwarf any similarly slow heterogeneous reaction. The Cr reaction was studied in an, essentially wall-less, HTP (high-temperature photochemistry) reactor[47] where no wall reaction could affect the measurements. The "nearest neighbor" to Pb/O_2 is the very fast, exothermic Sn + O_2 abstraction reaction. Its $k(380-1840\ K) = 5.1 \times 10^{-13}$-$(T/K)^{0.79}$ exp(−437 K/*T*) cm^3 molecule^{-1} s^{-1},[49] which would also dominate any much slower heterogeneous reactions.

Conclusions

The Pb(6^3P_0) reactions with N_2O, Cl_2, and HCl have been studied. In the temperature domains investigated no curvature is evident in their Arrhenius plots. Three parameter fits $k(T) = AT^n \exp(-E/RT)$ have also been made but did not further improve the precision limits of the results. Many other metal oxidation reactions studied in this laboratory show the predicted[50] Arrhenius plot curvature, but these were usually studied over wider temperature ranges than was possible for the Pb reactions.

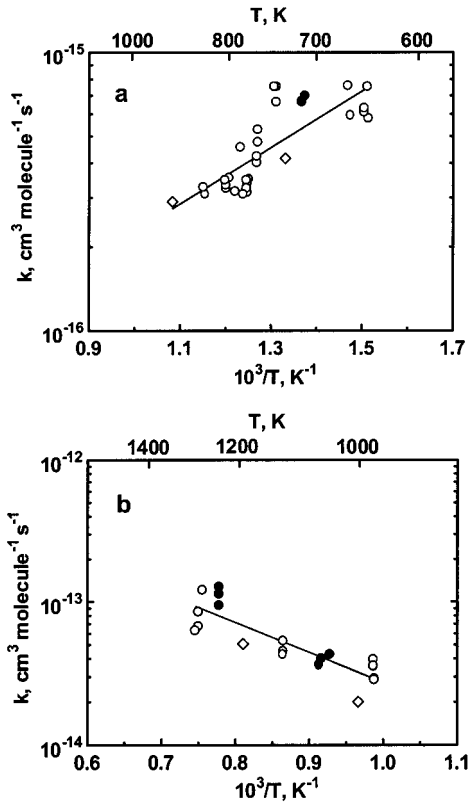

Figure 4. Arrhenius plots of the Pb + O_2 rate coefficients: (○) measurements taken using N_2 and quartz reaction tube; (●) measurements taken using Ar and quartz reaction tube; (◇) measurements taken using N_2 and mullite reaction tube; (—) best fits to the measurements at (a) 660−920 and (b) 1010−1340 K.

The Pb/O_2 system appears dominated by heterogeneous processes, and the apparent rate coefficient values obtained should be considered as phenomenological for the reactor used. In the combustion of solids such processes would dominate for the combination of these reactants. Further studies of homogeneous reactions of this system would require the use of reactors that operate essentially wall free. Such an environment can be provided for example at lower temperatures by the equipment in Husain's laboratory,[7−10] from 300 to 1800 K in an HTP reactor,[15,16,47] or in a shock tube.

Supporting Information Available: Tables 4S and 5S. This material is available free of charge via the Internet at http://pubs.acs.org.

Acknowledgment. This work was supported under NSF Grants CTS-9905265 and CTS-9632492, Dr. Farley Fisher, Program Director. We also thank William Flaherty, Charles Fung, and Christine Brown for dedicated assistance.

References and Notes

(1) Linak, W. P.; Srivastava, R. K.; Wendt, J. O. L. *Combust. Flame* **1995**, *100*, 241.

(2) Buckley, S. G.; Sawyer, R. F.; Koshland, C. P.; Lucas, D. *First United States Section Meeting of the Combustion Institute*; The Combustion Institute: Pittsburgh, PA, 1999; p 877.

(3) Saxena, S. C.; Jotshi, C. *Prog. Energy Combust. Sci.* **1996**, *22*, 401.

(4) Bell, C. F.; Husain, D. *J. Photochem.* **1985**, *29*, 267.

(5) Husain, D.; Littler, J. G. F. *J. Photochem.* **1973/74**, *2*, 247.

(6) Cross, P. J.; Husain, D. *J. Photochem.* **1977**, *7*, 157.

(7) Husain, D.; Sealy, I. P. *J. Photochem.* **1986**, *34*, 245.

(8) Husain, D.; Sealy, I. P. *J. Photochem.* **1985**, *30*, 387.

(9) Husain, D.; Sealy, I. P. *J. Photochem.* **1986**, *35*, 259.

(10) Husain, D.; Littler, J. G. F. *Combust. Flame*, **1974**, *22*, 295. These authors do not give the temperature range for the O_2 reaction. Presumably it was the same as for the NO data shown.

(11) Ryason, P. R.; Smith, E. A. *J. Phys. Chem.* **1971**, *75*, 2259.

(12) Unless otherwise indicated the ΔH_{298} values were based on: Chase, M. W., Jr. *NIST-JANAF Thermochemical Tables*; *J. Phys. Chem. Ref. Data* **1998**, Monograph 9.

(13) Belyung, D. P.; Futerko, P. M.; Fontijn, A. *J. Chem. Phys.* **1995**, *102*, 155.

(14) Blue, A. S.; Belyung, D. P.; Fontijn, A. *J. Chem. Phys.* **1997**, *107*, 3791.

(15) Fontijn, A. *Pure Appl. Chem.* **1998**, *70*, 469.

(16) Fontijn, A.; Futerko, P. M. In *Gas-Phase Metal Reactions*; Fontijn, A., Ed.; North-Holland: Amsterdam, 1992; Chapter 6.

(17) Slavejkov, A. G.; Futerko, P. M.; Fontijn, A. *23rd Symp. (Int.) Combust.*; The Combustion Institute: Pittsburgh, PA, 1990; p 155.

(18) Fontijn, A.; Felder, W. In *Reactive Intermediates in the Gas-Phase: Generation and Monitoring*; Setser, D. W., Ed.; Academic Press: New York. 1979; Chapter 2.

(19) Slavejkov, A.; Stanton, C. T.; Fontijn, A. *J. Phys. Chem.* **1990**, *94*, 3347.

(20) Irvin, J. A.; Quickenden, I. T. *J. Chem. Educ.* **1983**, *60*, 711.

(21) Felder, W.; Fontijn, A. *J. Chem. Phys.* **1978**, *69*, 1112, and references discussed therein.

(22) Futerko, P. M.; Slavejkov, A. G.; Fontijn, A. *J. Phys. Chem.* **1993**, *97*, 11950.

(23) STANJAN (Reynolds, W. C. *The Element Potential Method for Chemical Equilibrium Analysis; Implementation in the Interactive Program STANJAN*; Department of Mechanical Engineering, Stanford University, January 1986) calculation indicated that the use of N_2 allowed heating to roughly 200 K higher than with Ar for the same equilibrium dissociation.

(24) It has been previously shown[19,21,34] that at typical reaction times used in HTFFRs oxidants such as N_2O, Cl_2, and HCl can be used at temperatures several hundred kelvin higher than equilibrium dissociation would indicate. This can be attributed to kinetic constraints on the dissociation process.

(25) Press, W. H.; Flannery, B. P.; Teukolsky, S. A.; Vetterling, W. T. *Numerical Recipes*; Cambridge University: Cambridge, 1986; Chapter 14.

(26) Wentworth, W. E. *J. Chem. Educ.* **1965**, *42*, 96, 162.

(27) Ferguson, E. E.; Fehsenfeld, F. C.; Schmeltekopf, A. L. *Adv. At. Mol. Phys.* **1969**, *5*, 1.

(28) Fontijn, A.; Felder, W. *J. Phys. Chem.* **1979**, *83*, 24.

(29) Fontijn, A.; Felder, W. *J. Chem. Phys.* **1980**, *72*, 4315, and references discussed therein.

(30) Pearse, R. W. B.; Gaydon, A. G. *The Identification of Molecular Spectra*, 4th ed.; John Wiley & Sons: New York, 1976.

(31) Fontijn, A.; Blue, A. S.; Narayan, A. S.; Bajaj, P. J. *Combust. Sci. Technol.* **1994**, *101*, 59.

(32) Narayan, A. S.; Futerko, P. M.; Fontijn, A. *J. Phys. Chem.* **1992**, *96*, 290.

(33) This is the Reynolds number for flow to fully develop in a tube, where a is tube radius and ν bath gas viscosity; see: Potter, M. C.; Foss, J. F. *Fluid Mechanics*; Great Lake Press: Okemos, MI, 1982; p 274.

(34) Rogowski, D. F.; Marshall, P.; Fontijn, A. *J. Phys. Chem.* **1989**, *93*, 1118.

(35) Vinckier, C.; Christaensen, P. *J. Phys. Chem.* **1992**, *96*, 8423.

(36) Campbell, M. L. *J. Phys. Chem.* **1993**, *97*, 3922.

(37) Vinckier, C.; Verhaele, T.; Vanhees, I. *J. Chem. Soc., Faraday Trans.* **1996**, *92*, 1455.

(38) Helmer, M.; Plane, J. M. C. *J. Chem. Phys.* **1993**, *99*, 7696.

(39) Plane, J. M. C.; Rajasekhar, B.; Bartolotti, L. *J. Chem. Phys.* **1989**, *91*, 6177.

(40) Husain, D.; Marshall, P. *Int. J. Chem. Kinet.* **1986**, *18*, 83.

(41) Plane, J. M. C.; Saltzman, E. S. *J. Chem. Phys.* **1987**, *87*, 4606.

(42) Belyung, D. P.; Hranisavljevic, J.; Kashireninov, O. E.; Santana, G. M.; Fontijn, A.; Marshall, P. *J. Phys. Chem.* **1996**, *100*, 17835.

(43) Hranisavljevic, J.; Fontijn, A. *J. Phys. Chem.* **1997**, *101*, 2323.

(44) Hranisavljevic, J. Ph.D. Thesis, Rensselaer Polytechnic Institute, 1997; p 123.

(45) Golomb, D.; Best, G. T. *Trans. AGU* **1974**, *55*, 366.

(46) Oldenborg, R. C.; Dickson, C. R.; Zare, R. N. *J. Mol. Spectrosc.* **1975**, *58*, 283.

(47) Narayan, A. S.; Slavejkov, A. G.; Fontijn, A. *24th Symp. (Int.) Combust.*; The Combustion Institute: Pittsburgh, PA, 1992; p 727.

(48) Belyung, D. P.; Fontijn, A. *J. Phys. Chem.* **1995**, *99*, 12225.

(49) Fontijn, A.; Bajaj, P. N. *J. Phys. Chem.* **1996**, *100*, 7085.

(50) Fontijn, A.; Zellner, R. In *Reaction of Small Transient Species. Kinetics and Energetics*; Fontijn, A., Clyne, M. A. A., Eds.; Academic Press: London, 1983; Chapter 1.